REDUCING LETID WITH AN ADJUSTMENT OF THE ALOX-SINY:H LAYER SYSTEM

Andreas Schmid, Christian Fischer, Daniel Skorka, Annika Zuschlag, Giso Hahn
University of Konstanz, Department of Physics, 78457 Konstanz, Germany
andreas.schmid@uni-konstanz.de, Tel: +49 7531 882082, Fax: +49 7531 883895

ABSTRACT: Light and elevated temperature induced degradation (LeTID) negatively impacts the lifetime and electronic characteristics of silicon (Si) solar cells. Even though the exact underlying mechanism of LeTID and subsequent regeneration are still unknown, LeTID formation seems to depend on the hydrogen content in the Si bulk. In this study, we compare the LeTID and subsequent regeneration behaviour of p-type Cz-Si and mc-Si samples with different AlO_x/SiN_y:H passivation layer systems under illumination (1 sun) and elevated temperature (130°C). Provided that atomic layer deposited AlO_x can serve as diffusion barrier for hydrogen diffusing in the Si bulk from the SiN_y:H layer during firing, we are able to change the hydrogen content by adjusting the AlO_x layer thickness between 0 and 25 nm. Thus, we are able to show a reduction of LeTID by an adapted processing sequence without any losses in material quality.
Keywords: Degradation, Hydrogen, Diffusion, Silicon-Nitride, AlO_x, c-Si

1 INTRODUCTION

Light and elevated temperature induced degradation (LeTID) negatively impacts the lifetime and electronic characteristics of silicon (Si) solar cells [1-3]. Especially devices using the high efficiency passivated emitter and rear cell (PERC) technology are affected, and underlying mechanisms of LeTID are still largely unknown. Latest studies assume hydrogen to be a possible root cause for LeTID [4-9], although the true nature of the involvement of hydrogen remains unknown. In [3], it could be shown that LeTID was only observed on samples passivated with hydrogen containing dielectric layers, such as the hydrogen-rich PECVD SiN_y:H layer used in this work. As AlO_x can serve as diffusion barrier for hydrogen [10] during firing of the SiN_y:H layer, we should be able to vary the hydrogen content diffusing into the Si bulk by applying an adapted AlO_x layer between SiN_y:H and the Si wafer.

2 EXPERIMENTAL

Boron-doped high performance multicrystalline (hp mc) and Czochralski (Cz) grown Si sister wafers (5x5 cm^2) were processed to investigate the influence of different passivation layer systems on LeTID and following regeneration. A simplified scheme of the applied process sequence is given in Fig. 1. All wafers were etched in a solution of HNO_3 (65%), acetic acid (99.8%) and HF (50%) in a ratio of 15:2.5:1 to remove saw damage. Thereafter, an oxide was grown wet-chemically in a solution of H_2O_2 (30%) and H_2SO_4 (96%) in a ratio of 1:3 at about 80°C, which was afterwards stripped in diluted HF (3%) to remove surface contamination (Piranha clean). Afterwards, the samples were deposited using double-sided atomic layer deposition (ALD) AlO_x at 300°C. The layer thickness was varied between 5 and 25 nm and therefore the deposition time differed between several minutes and one hour. As deposition time at 300°C might play a role for the later observed LeTID kinetics, another set of samples was processed where the temperature load at 300°C was identical (31.5 min per side), and only the AlO_x layer thickness was varied (samples labelled "with time adjustment"). Furthermore, some samples were exposed 24 h to 400°C under low pressure in N_2 atmosphere directly after AlO_x deposition, to potentially outgas hydrogen present in the AlO_x layer.

All samples then received a 75 nm thick SiN_y:H layer by plasma-enhanced chemical vapor deposition (PECVD) and were fired in a belt furnace at a set peak temperature of 800°C. To compare the initial effective excess minority charge carrier lifetime (τ_{eff}), the samples were measured by the photoconductance decay (PCD) method at room temperature with a *Sinton Lifetime Tester WCT-120* and by the spatially resolved, fast and self-calibrated time-resolved photoluminescence imaging (TR-PLI) method [11].

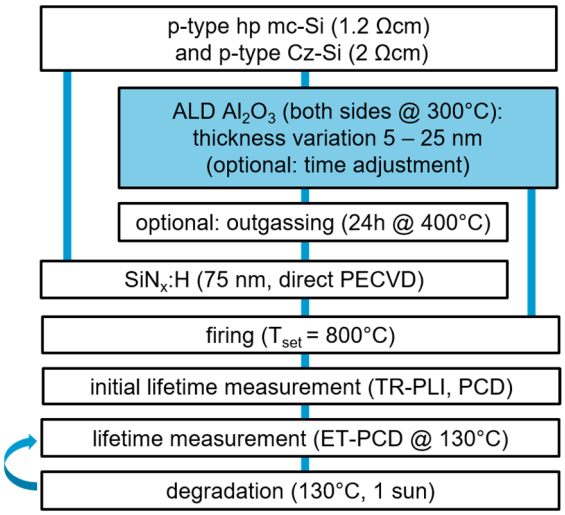

Figure 1: Simplified process sequence of the investigated lifetime samples.

For degradation and subsequent regeneration, the lifetime samples are held at a temperature of approx. 130°C under illumination with halogen lamps (1.0±0.1 suns) and τ_{eff} is measured repetitively via the PCD method at the elevated temperature of 130°C using a *Sinton Lifetime Tester WCT-120TS*. The lifetimes are extracted at a fixed excess charge carrier concentration of $\Delta n = 0.1 \times p_0$, where p_0 is the doping concentration of the investigated sample.

3 RESULTS AND DISCUSSION

As shown in Fig. 2, directly after the firing step the measured τ_{eff} values do not show an influence of the investigated AlO_x/SiN_y:H layer systems.

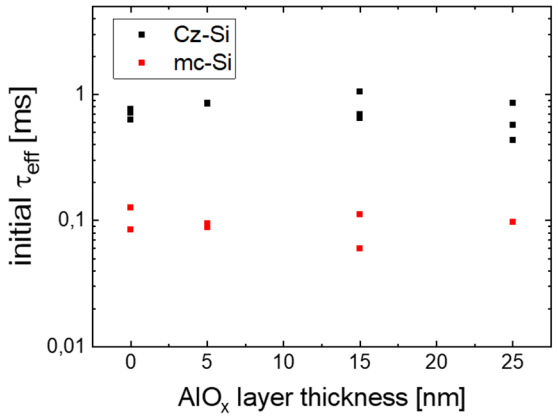

Figure 2: Initial τ_{eff} measured by PCD at room temperature and extracted at $\Delta n = 0.1 \times p_0$ of all mc-Si and Cz-Si samples with different AlO_x layers (0-25 nm) and subsequent SiN_y:H passivation.

Furthermore, spatially resolved TR-PLI lifetime maps confirm a homogeneous passivation. An example of a 25 nm AlO_x and subsequent 75 nm SiN_y:H passivated sample is shown in Fig. 3. This shows that no matter which passivation layer system is best regarding LeTID, it does not negatively affect the Si material quality.

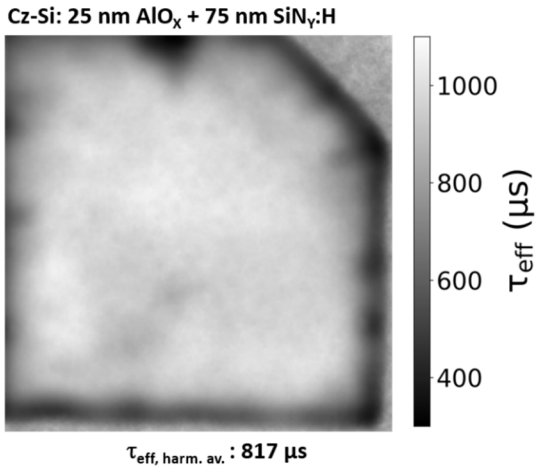

Figure 3: TR-PLI lifetime map at room temperature of a Cz-Si sample deposited with 25 nm AlO_x and 75 nm SiN_y:H shows a homogeneous passivation quality.

In order to allow better comparison of LeTID kinetics of various samples with varying τ_{eff} starting values, the lifetime equivalent defect density ΔN_{leq} is a suitable tool [12]. It is calculated using

$$\Delta N_{leq} = \frac{1}{\tau_{eff,t}} - \frac{1}{\tau_{eff,0}}$$

where $\tau_{eff,t}$ and $\tau_{eff,0}$ is the extracted lifetime measured by PCD at elevated temperature at any given time and in the initial state, respectively.

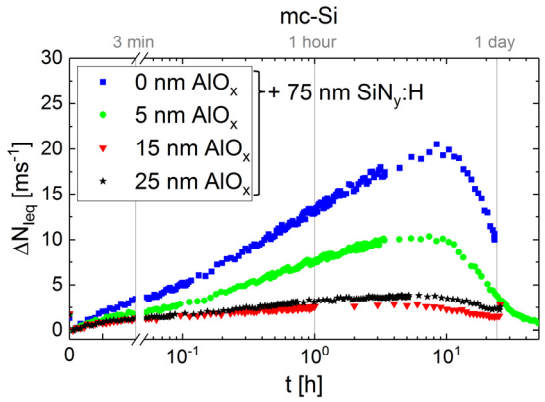

Figure 4: Time-dependent lifetime equivalent defect density of mc-Si samples, passivated with AlO_x of different thickness and subsequent 75 nm SiN_y:H after firing. Data calculated with extracted PCD lifetimes at elevated temperature at $\Delta n = 0.1 \times p_0$. As the 0 nm AlO_x sample (processed as standard) broke during characterization, the 0 nm AlO_x sample with additional time adjustment is shown here.

Fig. 4 exemplary shows time-dependent ΔN_{leq} values of the mc-Si samples passivated with 0-25 nm AlO_x and subsequent 75 nm SiN_y:H without time adjustment. As the as standard processed sample with 0 nm AlO_x broke during characterization, ΔN_{leq} values of the sample with additional time adjustment are shown instead. All samples show the typical LeTID and subsequent regeneration behaviour for mc-Si wafers at 130°C and one sun illumination. ΔN_{leq} increases in the first few hours until it reaches its maximum value after about eight to ten hours, followed by a decrease of ΔN_{leq}. It can be seen that an intermediate AlO_x layer with only 5 nm thickness leads to a decrease of the maximum value of lifetime equivalent defect density $\Delta N_{leq,\,max}$ from 20 ms^{-1} to 10 ms^{-1}. Increasing the layer thickness up to 15 nm further lowers $\Delta N_{leq,\,max}$ to less than 5 ms^{-1}. Interestingly, the value cannot be decreased further with even thicker layers, which possibly indicates a threshold value of AlO_x, regarding the hydrogen diffusion originating from the SiN_y:H layer, assuming that hydrogen is the trigger for the extent of observable LeTID.

For a better overview, $\Delta N_{leq,\,max}$ of all investigated samples are shown in Fig. 5. Even though $\Delta N_{leq,\,max}$ values in Cz-Si are roughly one order of magnitude below the values detected in mc-Si, the described observations above hold true for both Si materials. Moreover, samples without a final SiN_y:H layer (blue stars in Fig. 5), show comparable $\Delta N_{leq,\,max}$ values to the comparable samples with an AlO_x/SiN_y:H layer system. This further confirms the assumption of a threshold value of AlO_x thickness, regarding the hydrogen diffusion.

Samples with time adjustment during deposition (cf. red triangles in Fig. 5) as well as samples with outgassing of hydrogen (cf. green triangles in Fig. 5) are also investigated regarding their LeTID behaviour. As both process variations show comparable results to the standard process (cf. black squares in Fig. 5), an influence of the deposition time or the hydrogen content in the AlO_x layer itself can be excluded (presumed that the "outgassing" step led to a lower H concentration in the AlO_x layer).

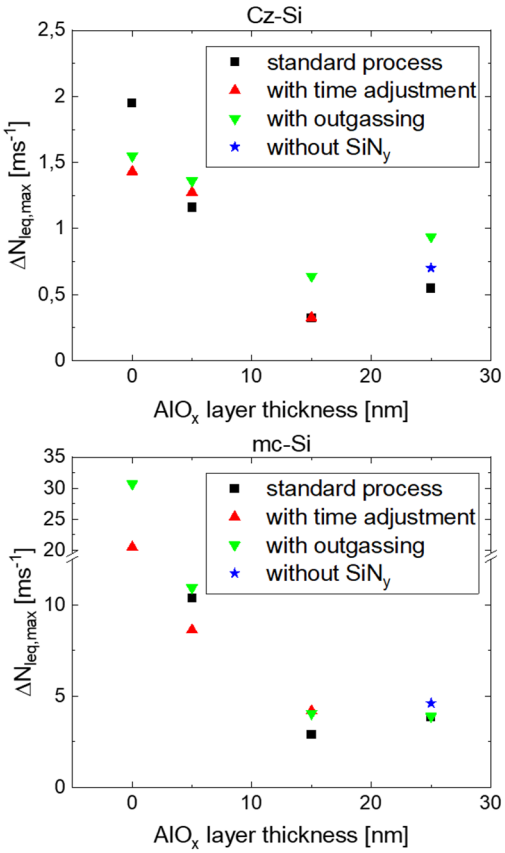

Figure 5: Maximum values of the lifetime equivalent defect density of mc (top) and Cz-Si samples (bottom) depending on the AlO_x layer thickness. The effective lifetime was extracted from PCD measurements at elevated temperature at an injection of $\Delta n = 0.1 \times p_0$. In addition to the standard process (black squares), a time adjustment of the AlO_x deposition (red triangles) and an outgassing of hydrogen after the AlO_x deposition (green triangles) was applied. The blue stars represent samples without a final SiN_y layer.

In various studies [13-15] it is shown, that LeTID is dependent on the firing temperature. Therefore, temperature profiles were measured via a thermocouple that is pressed on top of a wafer. It could be seen, that the temperature profiles do not change with varying AlO_x thickness within the AlO_x/SiN_Y:H layer system. Regarding the sample peak temperatures of the Cz-Si wafers shown in Fig. 6, it can be seen, that all temperatures of samples with an AlO_x/SiN_y:H layer system are within the range of

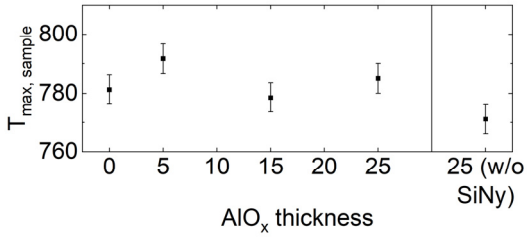

Figure 6: Measured sample peak temperatures during fast firing plotted against the AlO_x thickness within the AlO_x/SiN_Y:H layer system. Set peak temperature of the belt furnace was 800°C.

780 to 790°C and the peak temperature of the sample without a final SiN_y:H layer is slightly lower at about 770°C. Comparing these temperature differences with literature [13-15], the change of ΔN_{leq} observed in this study cannot be explained by the slightly different detected sample peak temperature during firing.

4 CONCLUSION

The influence of different AlO_x/SiN_y:H layer systems on LeTID strength and kinetics was investigated on mc-Si as well as Cz-Si wafers using τ_{eff} data from TR-PLI and PCD. Spatially resolved τ_{eff} measurements confirmed a homogeneous passivation quality for all samples, while injection dependent measurements showed no influence of the AlO_x layer thickness on τ_{eff}.

A comparison of calculated $\Delta N_{leq,\,max}$ values of both, mc and Cz-Si wafers showed a decrease of LeTID strength with an increase of AlO_x layer thickness up to 15 nm within the AlO_x/SiN_y:H layer system. Above 15 nm AlO_x thickness, $\Delta N_{leq,\,max}$ remains constant. This finding could be explained by assuming a threshold value of AlO_x layer thickness regarding hydrogen diffusion from the SiN_y:H layer through the AlO_x layer into the crystalline silicon wafer. It could be shown, that the different surface passivation layers used here do not impact the firing profile (peak firing wafer temperature) and thus the sample temperatures during firing are not responsible for the observed change in ΔN_{leq}. Furthermore, influences of the hydrogen content in the AlO_x layer itself as well as the ALD AlO_x deposition duration on ΔN_{leq} could be excluded (under the assumption that the "outgassing" step at 400°C for 24 h leads to a reduction of H concentration in the AlO_x layer).

These results help explain why the surface passivation step can affect LeTID, and ultimately why LeTID varies so strongly in PERC solar cells as different manufacturers use different AlO_x/SiN_y:H layer systems. Finally, it is possible to significantly reduce the LeTID defect density by an adapted processing sequence in PERC solar cells.

5 ACKNOWLEDGEMENTS

Part of this work was supported by the German BMWi under contract 0324204B. The content of the publication is the responsibility of the authors. The authors would like to thank L. Mahlstaedt, B. Rettenmaier and J. Engelhardt for technical support.

6 REFERENCES

[1] K. Ramspeck, S. Zimmermann, H. Nagel, A. Metz, Y. Gassenbauer, B. Birkmann, A. Seidl, *Proc. 27th EUPVSEC*, 861-865 (2012).
[2] A. Zuschlag, D. Skorka, G. Hahn, *Prog. Photovolt: Res. Appl.* 25, 545-552 (2017).
[3] F. Kersten, J. Heitmann, J.W. Müller, *Energy Procedia* 92, 828–832 (2016).
[4] D. Chen, P.H. Hamer, M. Kim, T.H. Fung, G. Bourret-Sicotte, S. Liu, C.E. Chan, A. Ciesla, R. Chen, M.D. Abbott, B.J. Hallam, S.R. Wenham, *Sol. Energ. Mat. Sol. Cells* 185, 174-182 (2018).

[5] A. Ciesla, S. Wenham, R. Chen, C. Chan, D. Chen, B. Hallam, D. Payne, T. Fung, M. Kim, S. Liu, S. Wang, K. Kim, A. Samadi, C. Sen, C. Vargas, U. Varshney, B.V. Stefani, P. Hamer, G. Bourret-Sicotte, N. Nampalli, Z. Hameiri, C. Chong, M. Abbott, *WCPEC-7* (2018).
[6] C. Vargas, K. Kim, G. Coletti,, D. Payne, C. Chan, S. Wenham, Z. Hameiri, *Proc. 33rd EUPVSEC*, 561-564 (2017).
[7] T. Fung, M. Kim, D. Chen, A. Samadi, C.E. Chan, B.J. Hallam, S. Wenham, M. Abbott, *AIP Conference Proceeding* 1999, 130004 (2018).
[8] J. Lindroos, A. Zuschlag, D. Skorka, G. Hahn, *IEEE J. Photovolt.* 10(1), 8-18 (2020).
[9] M.A. Jensen, A. Zuschlag, S. Wieghold, D. Skorka, A.E. Morishige, G. Hahn, T. Buonassisi, *J. Appl. Phys.* 124(8), 085701 (2018).
[10] A.A. Dameron, S.D. Davidson, B.B. Burton, P.F. Carcia, R.S. McLean, S.M. George, *J. Phys. Chem. C*, 112, 4573-4580 (2008).
[11] D. Kiliani, A. Herguth, G. Micard, J. Ebser, G. Hahn, *Sol. Energ. Mat. Sol. Cells* 106, 55-59 (2012).
[12] A. Herguth, *IEEE J. Photovolt* 9(5), 1182-1194 (2019).
[13] D. Chen, M. Kim, B. V. Stefani, B. J. Hallam, M. D. Abbott, C. E. Chen, R. Chen, D. N. Payne, N. Nampali, A. Ciesla, T. H. Fung, K. Kim, S. R. Wenham, *Sol. Energ. Mat. Sol. Cells* 172, 293-300 (2017).
[14] T. Niewelt, M. Selinger, N. E. Grant, W. Kwapil, J. D. Murphy, M. C. Schubert, *J. Appl. Phys.* 121, 185702 (2017).
[15] D. Bredemeier, D. Walter, S. Herlufsen, J. Schmidt, *AIP Advances* 6, 035119 (2016).